J. Biochem. **142,** 707–713 (2007)
doi:10.1093/jb/mvm187

Effect of N-terminal Residues on the Structural Stability of Recombinant Horse L-chain Apoferritin in an Acidic Environment

Keiko Yoshizawa[1,2], Yumiko Mishima[1,2], Sam-Yong Park[3], Jonathan G. Heddle[1,3], Jeremy R. H. Tame[3], Kenji Iwahori[1,2], Mime Kobayashi[1,2] and Ichiro Yamashita[1,2,*]

[1]CREST, Japan Science and Technology Agency, 4-1-8 Honcho, Kawaguchi, Saitama, 332-0012; [2]Graduate School of Materials Science, Nara Institute of Science and Technology, 8916-5 Takayama, Ikoma, Nara 630-0192; and [3]Protein Design Laboratory, Yokohama City University, 1-7-29 Suehiro-cho, Tsurumi-ku, Yokohama, Kanagawa, 230-0045, Japan

Received September 3, 2007; accepted September 14, 2007; published online October 15, 2007

The denaturation of recombinant horse L-chain apoferritin (rLF), which is composed of 24 L-chain subunits, in acidic solution was studied. Using two rLF mutants, lacking four (Fer4) or eight (Fer8) N-terminal amino acid residues, the effect of N-terminal residues on the protein's stability was investigated. Of the two mutants and wild-type rLF, the tertiary and secondary structures of Fer8 were found to be most sensitive to an acidic environment. The Fer8 protein dissociated easily into subunit dimers at or below pH 2.0. Comparing the crystal structures of the mutant proteins, deletion of the N-terminal residues was found to result in fewer inter- and intra-subunit hydrogen bonds. The loss of these bonds is assumed to be responsible for lower endurance against acidic denaturation in N-terminus-deleted mutants. These results indicated that the inter- and intra-subunit hydrogen bonds of N-terminal residues affect the denaturation, especially oligomer formation of apoferritin subunits and will be of use in designing ferritin-based nanodevices.

Key words: acidic denaturation, apoferritin, ferritin, hydrogen bond, protein structure.

Abbreviations: rLF, recombinant horse L-chain apoferritin; rHF, recombinant horse H-chain apoferritin; CD, circular dichroism.

Ferritin is an iron storage protein supramolecule found in wide range of organisms and its structure and function have been investigated in detail (*1*). Apoferritin, ferritin without a ferrihydrite core, consists of 24 subunits that form a cage-shaped protein shell via non-covalent interactions. Mammalian ferritin is composed of H-chain (21 kDa) and L-chain (18 kDa) proteins in various proportions. A ferritin molecule has outer and inner diameters of ~12 nm and 7 nm, respectively. The H- and L-chains amino acid sequences share 55% homology and they share the same characteristic tertiary structure consisting of a bundle of four anti-parallel helices (A–D), a C-terminal short helix (E) and a long loop connecting helices (B and C). High-resolution X-ray crystallographic analysis of the horse spleen apoferritin structure have shown that the subunits are preferentially organized in dimeric building blocks, which are ideally suited to generate a molecular assembly, consisting of a protein shell with 4-3-2 symmetry and with inter-subunit channels along the 3-fold axes for the passage of iron ions (*2–6*).

Apoferritin is known to be highly resistant to chemical and physical denaturants, which makes it an intriguing supramolecule for applications that need harsh conditions (*7–9*). Horse spleen apoferritin, which consist of 90% L-chain and 10% H-chain, denatures only under extreme conditions such as temperatures >80°C (*10*) or at pH values below 2.8 (*11*). Denaturation by guanidine hydrochloride is strongly pH-dependent (*10*) and apoferritin can be reversibly dissociated and re-associated by various denaturants (*11*).

Recombinant H- and L-apoferritins (rHF and rLF), which are homopolymers composed of H- or L-chain subunits, have been generated to investigate their iron incorporation mechanism and their stabilities (*2*, *12*, *13*). The rLF apparently has greater stability against acidic condition and denaturants compared to rHF. By mutational studies using recombinant apoferritins, a specific salt bridge within the four-helix bundle between Lys59 and Glu104 in the L-chain has been implicated as the source of the higher stability. When mutations were introduced into rHF so that the protein gained the salt bridge, protein stability increased. At the same time, both intra- and inter-chain contacts are found to be essential for protein stability (*6*, *14*, *15*). While mutating the residues exposed to solvent and not involved in inter- and intra-chain interactions had no effect on stability, deletion of the N-terminal extension Thr1-His13, which is involved in intra- and inter-chains interactions of rHF, significantly reduced the protein's stability (*14*).

Due to its structural stability, rLF has been used for applications in nanotechnology (*7*, *8*). We and others

*To whom correspondence should be addressed. Tel: +81-743-72-6135, Fax: +81-743-72-6196, E-mail: ichiro@ms.naist.jp

have reported the construction of mutant rLFs with functional peptides attached to their N-terminus aiming at future application of functional nano-structures in electronic devices and biosensors (*16–20*). Considering the structural similarity between H- and L-chain subunits, it is important to investigate the effect of N-terminal residues of rLF on its structural stability.

In this article, using two mutant rLFs lacking their four (Fer4) or eight (Fer8) N-terminal amino acid residues, the effect of N-terminal residues on the stability of rLF against acidic pH was studied. X-ray crystallographic analysis of the mutant rLFs revealed that the inter- and intra-subunit hydrogen bonds within N-terminal residues affect the structural stability of the protein at low pH. Particularly, residues Ile5-Asn8 was found to be critical for stability of the oligomer structure.

MATERIALS AND METHODS

Construction of Recombinant L-chain Apoferritin Plasmid DNA—Expression plasmid pKIT0, which encodes the full length amino acids (1–175) of horse L-chain apoferritin subunit has been described (*21*, *22*). The pKIT4 (Fer4) and pKIT8 (Fer 8) are designed to lack the first 4 and 8 N-terminal amino acids, respectively. Construction of pKIT8 has been described (*21*). For pKIT4, 12 base-pairs from the 5′ end were deleted from the PCR product of the L-chain apoferritin DNA fragment, and ligated into *Eco*RI–*Hind*III digested pMK2 vector (*23*).

Purification and Characterization of L-chain Apoferritin Protein—NovaBlue competent cells (Novagen) were transformed with the plasmids, pKIT0, pKIT4 or pKIT8 and grown in LB medium for overnight at 37°C. Cells were recovered by centrifugation at 8,000 r.p.m. for 20 min, suspended in a small volume of Tris–HCl (pH 8.0) buffer, and lysed by ultrasonication (Sonifer 250; Branson Ultrasonic Corp., Danbury, CT, USA) for 30 times for 1 s with 1 s interval on ice. After centrifugation at 12,000 r.p.m. for 20 min, the supernatant was subjected to a thermal denaturation at 60°C for 15 min in a shaking water bath. After centrifugation at 12,000 r.p.m. for 20 min, the supernatant was loaded onto a Q-Sepharose column (Pharmacia) in Tris–HCl (pH 8.0) buffer and eluted with a 0–1 M NaCl linear gradient. Fractions containing ferritin protein were collected and concentrated via centrifuge filtration (Quantitative Molecular Weight Limit 150 kDa, Orbital Biosciences, Topsfield, MA, USA), then loaded onto a Sephacryl S-300 column (Pharmacia) equilibrated in 50 mM Tris–HCl (pH 8.0) buffer, 0.15 M NaCl. Protein purity was assessed by sodium dodecyl sulfate polyacrylamide gel electrophoresis (SDS-PAGE) followed by Coomassie Brilliant Blue staining. Cells carrying plasmids encoding Fer0, Fer4 and Fer8 mutant proteins produced the recombinant L-chain apoferritin, which consisted of residues 2–175, 5–175 and 9–175 amino acids, respectively.

Proteins were analysed by matrix-assisted laser desorption/ionization time-of-flight mass spectrometry (MALDI TOF MS; Applied Biosystems) to determine the molecular weights of the apoferritin subunits. The first methionine of Fer0 is known to be removed probably due to the post-translational modification (*16*). Fer4 and Fer8 proteins have an initiation methionine residue at their N-terminus. The observed molecular weights were 19,877.0 for Fer0, 19,659.0 for Fer4 and 19,150.0 for Fer8, which agreed well with the predicted molecular weights of 19,830.5, 19,659.5 and 19,147.9, respectively.

Denaturation and Dissociation Analysis of rLFs at Low pH—The rLF mutant proteins (1.0 mg/ml) were incubated for 10 min at 20°C in a HCl solution of pH between 7.0 and 1.0. A total of 1.0 mg/ml protein solution was found to equate to an optical density of 0.63 at 280 nm. An In-Lab 422 electrode (Mettler-Toledo AG) connected to a Corning P507 ion meter was used to measure pH value in the presence of the protein. The samples were then analysed by size-exclusion chromatography and circular dichroism (CD) spectroscopy.

Size-exclusion chromatography was carried out at 20°C on a TSK gel G3000SWxL PEEK column (TOSOH, Tokyo, Japan) equilibrated with 50 mM Tris–HCl (pH 8.0) containing 0.15 M NaCl at a flow rate of 1 ml/min controlled by a TOSOH dual pump. The size of protein was calibrated with horse spleen apoferritin (440 kDa, elution volume $Ve = 7.5$ ml), lgG (158 kDa, elution volume $Ve = 8.8$ ml), ovalbumin (45 kDa, elution volume $Ve = 9.8$ ml), Myoglobin (17kDa, elution volume $Ve = 11.4$ ml) and Vitamin B-12 (1.35 kDa, elution volume $Ve = 13.1$ ml).

CD spectra were recorded on a J-820 spectropolarimeter (JASCO, Tokyo, Japan). Far-UV (200–250 nm) and near-UV CD (250–300 nm) recordings were performed in a 0.1 cm and 1.0 cm path length quartz cuvette, respectively. The results are expressed as mean residue ellipticity ([θ]) using a mean amino acid residue weight of 110.

Crystallization and X-ray Diffraction of rLF Mutants—A 2 μl protein sample, equilibrated against 50 mM Tris–HCl (pH 8.0), was mixed with an equal amount of reservoir solution and crystallization was carried out at 293 K by the hanging drop vapour diffusion technique. Reservoir solutions used for each crystallization were as follows: Fer0 (16 mg/ml), 100 mM Tris–HCl (pH 7.5) containing 0.13% (w/v) $CdCl_2$, 15% polyethylene glycol #400 (PEG400), 190 mM $CaCl_2$ and 5% glycerol; Fer4 (9 mg/ml), 100 mM Tris–HCl (pH 7.5) containing 0.13% $CdCl_2$, 190 mM $CaCl_2$, 5% glycerol and 15% PEG400; Fer8 (10.6 mg/ml), 100 mM Tris–HCl (pH6.8) containing 225 mM ammonium sulphate, 0.13% $CdCl_2$ and 25% 2-Methyl-2,4-pentanediol.

Data at the temperature of liquid nitrogen were collected as 1.0 oscillation frames using a MAR CCD detector (*24*) at RIKEN beamline-2 (BL44B2) of the SPring8 Synchrotron in Harima, Japan. The collected images were processed with DENZO, and scaled with SCALEPACK (*25*).

Structure Determination and Refinement—Horse L-ferritin (Protein Data Bank entry 1AEW) (*15*) was used as a search model and the mutant ferritin structures were solved by molecular replacement using the MOLREP program (*26*, *27*). Refinement of the atomic coordinates and displacement parameters was carried out by the maximum likelihood method with the REFMAC program (*28*).

The model building was performed using the TURBO-FRODO program (*29*) on a Silicon Graphics Octane computer. The $|Fo| - |Fc|$ and $2|Fo| - |Fc|$ maps were

Table 1. **Data collection and refinement statistics.**

	Fer0	Fer4	Fer8
Crystal system			
Space group	*F* 4 3 2	*F* 4 3 2	*F* 4 3 2
Cell dimensions (Å),	$a=b=c=180.5$	$a=b=c=180.3$	$a=b=c=180.2$
(Degree)	$a=b=g=90$	$a=b=g=90$	$a=b=g=90$
Data collection			
Light source	SPring-8, BL44XU	SPring-8, BL44XU	SPring-8, BL44XU
Detector	Oxford CCD	Oxford CCD	Oxford CCD
Refinement			
Resolution (Å)	19.8–1.8	41.5–1.4	19.8–1.4
Used reflections			
($\|F\| > 2\ \|F\|$)	24,602	45,991	46,795
Completeness (%)	100	100	100
Residues	171 (S2∼L172)	170 (I5∼H174)	165 (T9∼K173)
Water	174	185	177
Cadmium ion	2	–	2
Average B-factor (Å2)	13.7	13.7	14.3
RMSD			
Bond length (Å)	0.011	0.011	0.008
Bond angle (degree)	1.23	1.20	1.11
R-factor (%)	19.7	22.3	22.1
Free-R (%)	22.5	24.2	23.9

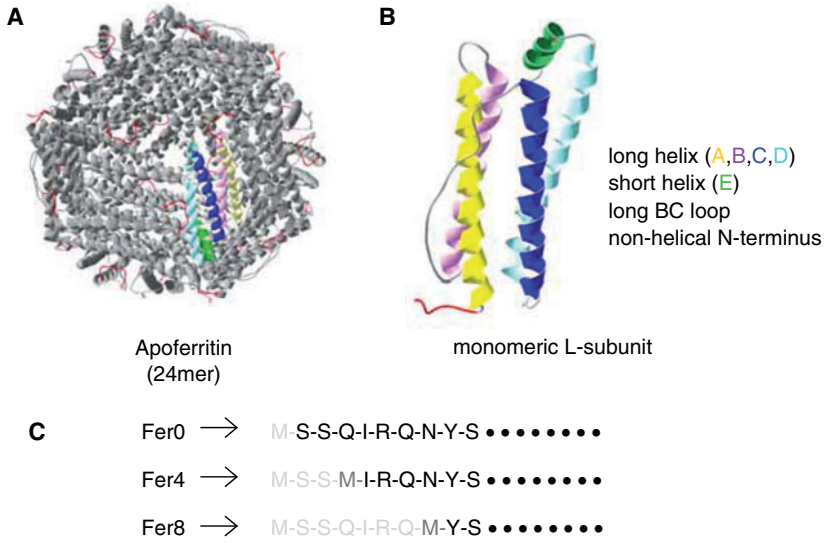

Fig. 1. **N-terminal residues of recombinant L-chain apoferritin (rLF) mutants.** Recombinant apoferritin consists of 24 L-chain subunits. (A) Crystal structure of L-chain apoferritin with a single subunit highlighted in colour and N-terminal residues in red. (B) Single L-ferritin subunit showing the tertiary structure. The N-terminal portion is highlighted in red. (C) N-terminal amino acid sequence of wild-type and mutant L-chain apoferritins. The first methionine residue of native L-ferritin (Fer0) is removed presumably by the result of post-translational modification (*16*).

used to locate the correct model. The model was refined by several rounds of positional and B-factor refinements, followed by manual model building. Water molecules were incorporated, where the difference in density exhibited values >3.0 σ above the mean and the $2|Fo| - |Fc|$ map showed a density of >1.3 σ. The stereo quality of the model was assessed using the programs PROCHECK (*30*) and WHAT-CHECK (*31*). Data collection and refinement statistics are shown in Table 1. Atomic coordinates of Fer0, Fer4 and Fer8 have been deposited to Protein Data Bank under accession numbers 2ZA6, 2ZA7 and 2ZA8.

RESULTS AND DISCUSSION

Effect of N-terminal Residues on the Polymeric Structure of L-chain Apoferritin—The stability of the rLF protein at acidic pH and the effect of its N-terminal residues were studied. Wild-type and mutant proteins rLF (Δ1–4) and rLF (Δ1–8) were named Fer0, Fer4 and Fer8, respectively (Fig. 1). After incubation of each rLF mutant for 10 min at room temperature in the pH range 1.0–3.0, the proteins were analysed by size-exclusion chromatography. At pH values above 2.5, all rLF mutants maintained their quaternary structure

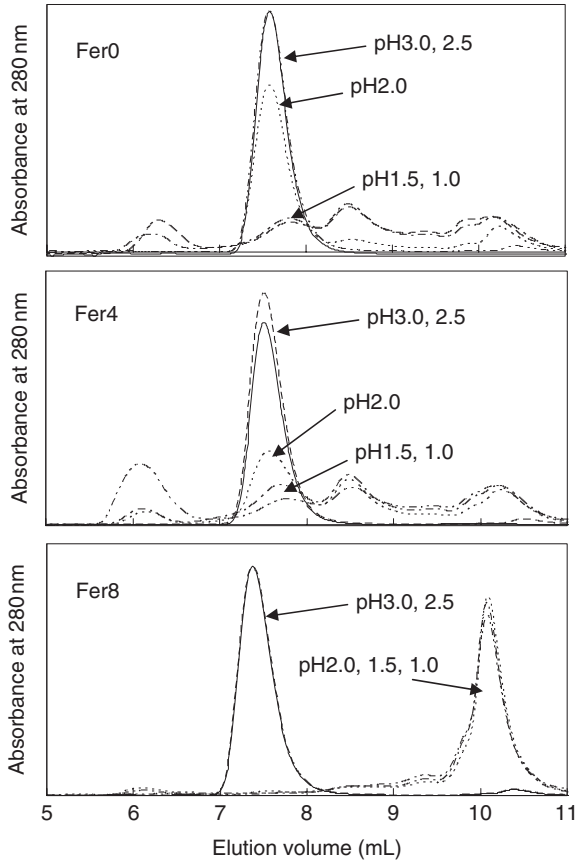

Fig. 2. **Effect of N-terminal residues on acidic denaturation of rLF mutants.** After rLFs mutant proteins were incubated for 10 min at respective pH values, the structure of the proteins were analysed by size-exclusion chromatography. Elution profiles at pH 3.0 (continuous line), pH 2.5, (dashed line), pH 2.0 (dotted line), pH 1.5 (dash dot dashed line) and pH 1.0 (dash double dot dashed line) are shown.

as judged from the elution volume (*Ve*) after TSKgel G3000SWXL PEEK column chromatography (Fig. 2). The *Ve* = 7.5 ml coincided with that of native rLF at pH 8.0. Upon incubation below pH 2.0, the quaternary structures dissociated leading to later elution time. Judging from the elution volume, the peak at *Ve* = 10.3 ml (36 kDa) corresponds to the size of the subunit dimer. At pH 2.0, most of the Fer8 protein dissociated into dimeric structures, while Fer0 and Fer4 maintained their polymeric structures (Fig. 2, dashed lines). At pH 1.5, Fer0 and Fer4 dissociated into several polymeric structures including subunit dimers and tetramers. On the other hand, Fer8, almost exclusively, dissociated into dimers (*Ve* = 10.2 ml) at or below pH 2.0 and the dimers did not dissociate even at pH 1.0. The result shows that N-terminal residues, especially Ile5-Gln8, contribute to the stability of the oligomeric structures of rLF.

Effect of N-terminal Residues on the Spectral Properties of L-chain Apoferritin Assessed by Circular Dichroic Spectra—The stability was next evaluated using CD. In the near-UV region, rLFs at pH 7.0 showed a characteristic spectrum with two positive peaks at 293 nm and 286 nm due to the immobilization of the tryptophan residues and of at least some of the tyrosines in a hydrophobic environment (Fig. 3A). L-chain apoferritin has only one tryptophan residue per subunit. The higher intensity of the 286 nm peak compared to the peak at 292 nm suggests an overlap with another CD peak. It could be due to tyrosine, whose CD maximum is known to occur around 277 nm with a 0–0 band about 6 nm towards red (*32*).

Weak ellipticity peaks found around 268 nm and 262 nm are attributed to phenylalanyl residues. In acidic denaturation, the near-UV CD spectra of Fer8 were markedly different from that of Fer0 and Fer4 probably due to the localization of many aromatic residues in the vicinity of the N-terminus or at the intra-subunit contacts. While spectral features of Fer0 and Fer4 gradually diminished, starting around pH 2.5 that of Fer8 was almost completely absent even at pH 2.5. At or below pH 1.5, their spectra were negative below 290 nm and weak peaks that can be attributed to phenylalanine were visible. Dichroic activity was absent over the entire spectral range, which indicate the exposure of the aromatic residues to solvent.

The CD spectra of three rLFs were also recorded in the far-UV region (Fig. 3B). At neutral pH, deletion of Ser2-Asn8 did not show any remarkable change and the molar ellipticity of rLFs was somewhat higher at 222 nm compared to the value at 208 nm. In acidic conditions, the ellipticity values at 222 nm become smaller than the value at 208 nm, indicating a decrease in the α-helix content. The spectra due to α-helices significantly decreased at or below pH 2.0 for Fer0 and Fer4. Loss of the α-helix signal was observed at pH 2.5, 0.5 units higher for Fer8. However, a great deal of ordered structures were still present in the subunit polypeptide even at pH 1.0.

N-terminal deletions apparently did not affect native 24mer structures including α-helix and tertiary structures but made the protein's spherical structure sensitive to acid denaturation.

The asymmetric environments of the tryptophans seemed to diminish, but a relatively weak negative CD spectrum in the tyrosyl and phenylalanyl region still remained. These marked tertiary changes, however, did not result in dissociation of dimers as judged by size exclusion chromatography.

Hydrogen Bonds Involving N-terminal Residues are Important for the Stability of rLF—From the crystal structure of rLF mutants, hydrophobic interactions of D-helix residues and extensive hydrogen bonding between N-terminal side- and main-chain atoms with those of residues in helices C and D of another subunit were found around the 2-fold and 3-fold axes (Fig. 4). The N-terminal residues Ser2-Asn8 are involved in both inter- and intra-chain interaction and the absence of the N-terminal region in mutants resulted in a decreased number of inter- and intra-subunit hydrogen bonds (Fig. 4). Many further interactions involving helices E and D and the DE turn around the 4-fold axis are also observed. The extensive cooperative network of inter- and intra-subunit interactions explains the unusual stability of ferritin and the observation that dissociation is accompanied by subunit unfolding (*33*).

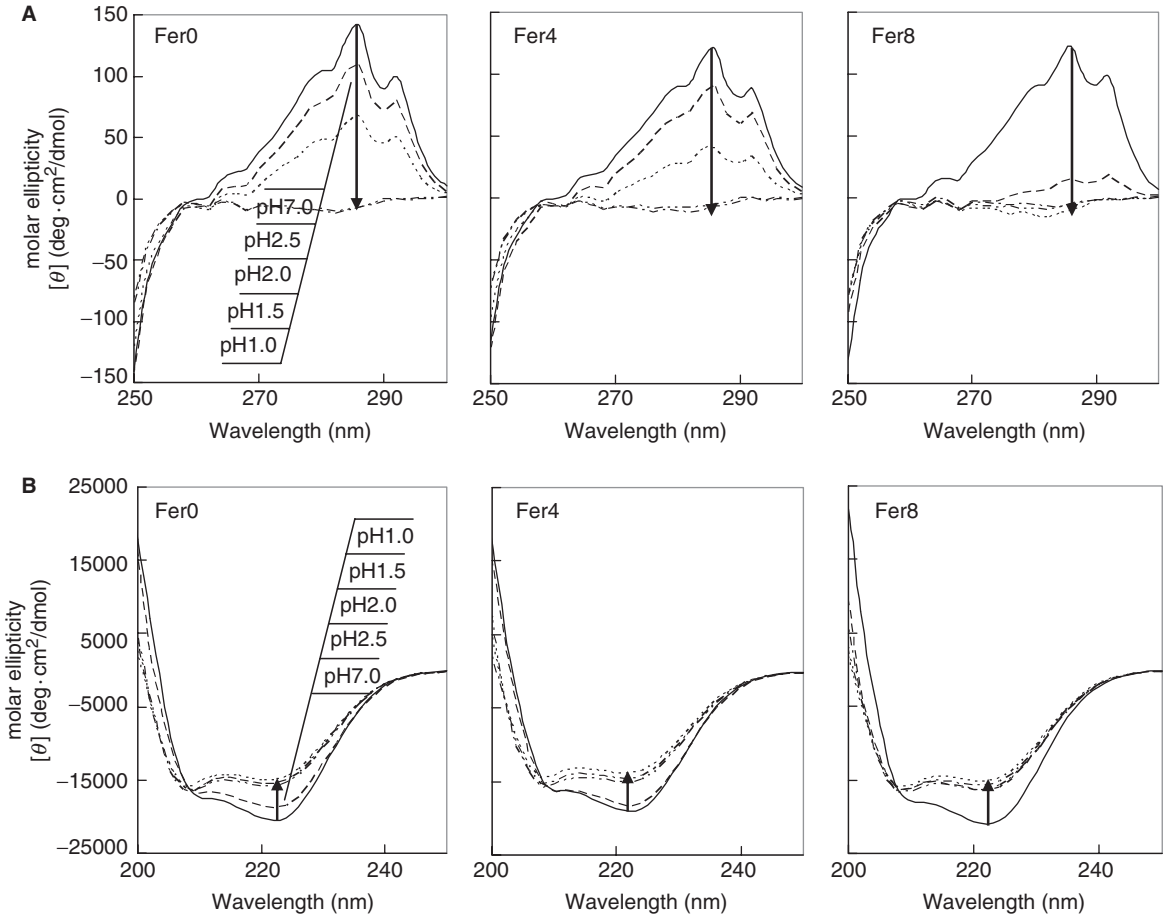

Fig. 3. **Acidic denaturation monitored by CD spectra.** Near-UV spectra (A) and far-UV spectra (B) of rLF mutants in acidic condition. Spectra at pH 7.0 (continuous line), pH 2.5 (dashed line), pH 2.0 (dotted line), pH 1.5 (dash dot dashed line) and pH 1.0 (dash double dot dashed line) are shown. Arrows in the figures indicate progressive decrease of the characteristic peaks [293 nm, 286 nm and 260–270 nm from aromatic residues in (A), and 222 nm and 208 nm from α-helix in (B)].

Analysis of the L-chain apoferritin 2-fold axial interface revealed the presence of a large number of hydrogen bonds, salt bridges and hydrophobic interactions (*6*). The structural information of mutant rLFs obtained by X-ray crystallography also showed that dimeric formation entails burying of several aromatic residues (*e.g.* Phe-38 and -79, Tyr-29). The results of near-UV CD spectroscopy suggest that the environment around phenylalanine and tyrosine are slightly preserved. In acidic conditions, the results suggest the presence of a quaternary assembly in the absence of a rigid tertiary structure and the formation of inter-subunit contacts may be preliminary to the formation of a compact hydrophobic core. It has been known that several proteins also adopt relatively compact, soluble conformational states that differ from the native structure and do not unfold completely as indicated by their CD spectroscopic properties (*34*).

N-terminal Residues are Important for the Inter-dimer Interaction of rLF—Although the α-helix content of Fer0 and Fer4 was decreased at pH 2.0 (Fig. 3B), the 24mer assemblage was maintained (Fig. 2). At pH 1.5, the 24mer dissociated into subunits (Fig. 2) and the Trp spectrum disappeared (Fig. 3A). For Fer8, those changes were observed at pH 2.5 and 2.0, respectively, 0.5 pH units higher than that observed in Fer0 and Fer4. There is only one Trp in the rLF subunits and it is located near the 4-fold interface. The fact that the disappearance of the tryptophanyl spectrum and dissociation of the 24mer into individual subunits were observed at around the same pH (Figs 2 and 3A) suggests that the loss of the interactions in the 4-fold interface leads to the dissociation of the 24mer assemblage. The observation that Fer0 and Fer4 molecules did not completely dissociate into subunits even at pH 1.0 (Fig. 2) indicates that intra-subunit 3-fold and 4-fold interactions are stabilized by the hydrogen bonds of the N-terminal 2–8 residues, which were not disturbed even in extreme acidic conditions (Fig. 4). Fer8 was dissociated more easily than Fer0 or Fer4 but Fer8 could still be reversibly assembled to form the 24mer assemblage at neutral pH as was the case for other native or recombinant apoferritins (data not shown). In conclusion, N-terminal residues, especially Ile5 - Asn8, contribute to stabilize the secondary and tertiary structures of the rLF subunit. The dimeric form of the subunit is highly stable and the N-terminal residues play an important

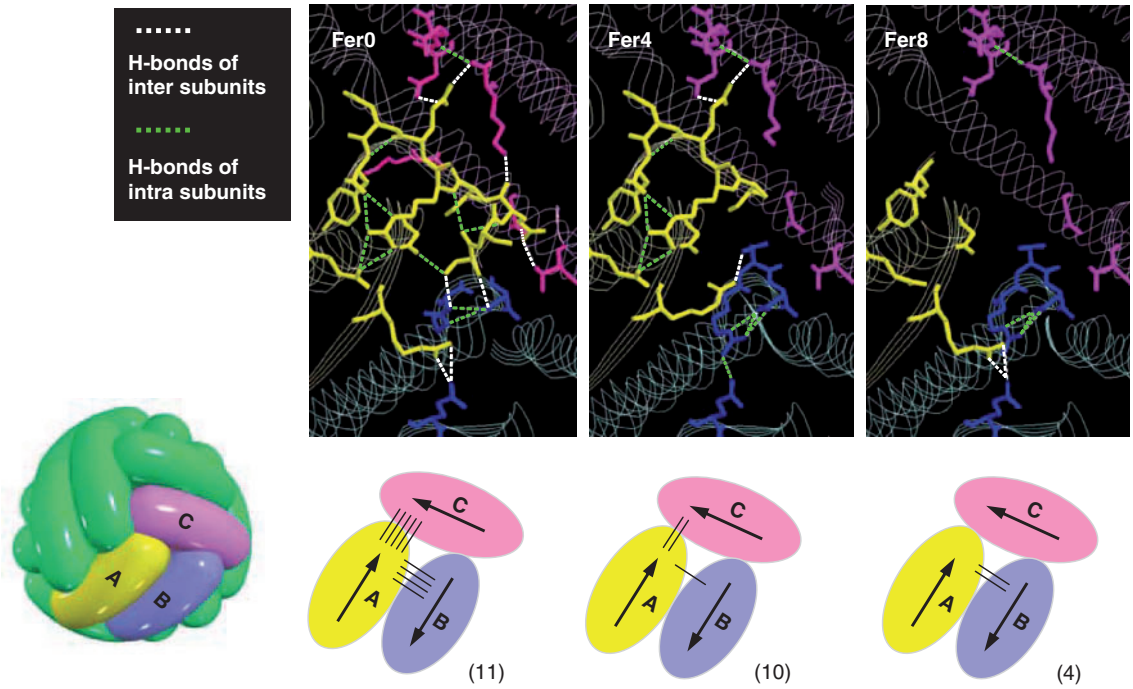

Fig. 4. **Structural comparison of mutant rLFs around the N-terminal region.** Residues that are involved in inter- and intra-subunit hydrogen bond around N-terminal region of mutant rLFs are highlighted in the upper figures created using TURBO-FRODO (*29*). Schematic representation of three subunits (A, B and C) is shown below. Yellow (A), magenta (B) and cyan (C) roughly correspond to the colours represented in the upper figures. Inter-subunit hydrogen bonds are depicted by solid lines and the number of intra-subunit hydrogen bonds is shown in parenthesis. Location of the three subunits is depicted in schematic representation of Appoferritin 24mer shown below left.

role for dimer–dimer interactions to retain the multimer structure of apoferritin.

REFERENCES

1. Massover, W.H. (1993) Ultrastructure of ferritin and apoferritin – a review. *Micron* **24**, 389–437
2. Lawson, D.M., Artymiuk, P.J., Yewdall, S.J., Smith, J.M.A., Livingstone, J.C., Treffry, A., Luzzago, A., Levi, S., Arosio, P., Cesareni, G., Thomas, C.D., Shaw, W.V., and Harrison, P.M. (1991) Solving the structure of human H ferritin by genetically engineering intermolecular crystal contacts. *Nature* **349**, 541–544
3. Rice, D.W., Ford, G.C., White, J.L., Smith, J.M., and Harrison, P.M. (1983) The spatial structure of horse spleen apoferritin. *Adv. Inorg. Biochem.* **5**, 39–50
4. Clegg, G.A., Standfield, R.F. D., Bourne, P.E., and Harrison, P.M. (1980) The structure and heavy-metal-ion-binding sites of horse spleen apoferritin. *Biochem. Soc. Trans.* **8**, 654–655
5. Clegg, G.A., Fitton, J.E., Harrison, P.M., and Treffry, A. (1980) Ferritin: molecular structure and ironstorage mechanisms. *Prog. Biophys. Mol. Biol.* **36**, 56–86
6. Gallois, B., d'Estaintot, B.L., Michaux, M.A., Dautant, A., Granier, T., Précigoux, G., Soruco, J.A., Roland, F., Chavas-Alba, O., Herbas, A., and Crichton, R.R. (1997) X-ray structure of recombinant horse l-chain apoferritin at 2.0 Å resolution: implications for stability and function. *J. Biol. Inorg. Chem.* **2**, 360–367
7. Yoshimura, H., Scheybani, T., Baumeister, W., and Nagayama, K. (1994) Two-dimensional protein array growth in thin layers of protein solution on aqueous subphases. *Langmuir* **10**, 3290–3295
8. Yamashita, I. (2001) Fabrication of a two dimensional array of nano-particles using ferritin. *Thin Solid Films* **393**, 12–18
9. Douglas, T., Dickson, D.P. E., Betteridge, S., Charnock, J., Garner, C.D., and Mann, S. (1995) Synthesis and structure of an iron(III) sulfide-ferritin bioinorganic nanocomposite. *Science* **269**, 54–59
10. Listowsky, I., Blauer, G., Englard, S., and Betheil, J.J. (1972) Denaturation of horse spleen ferritin in aqueous guanidinium chloride solutions. *Biochemistry* **11**, 2176–2182
11. Crichton, R.R. and Bryce, C.F. A. (1973) Subunit interactions in horse spleen apoferritin. Dissociation by extremes of pH. *Biochem. J.* **133**, 289–299
12. Levi, S., Luzzago, A., Cesareni, G., Cozzi, A., Franceschinelli, F., Albertini, A., and Arosio, P. (1988) Mechanism of ferritin iron uptake: activity of the H-chain and deletion mapping of the ferro-oxidase site. A study of iron uptake and ferro-oxidase activity of human liver, recombinant H-chain ferritins, and of two H-chain deletion mutants. *J. Biol. Chem.* **263**, 18086–18092
13. Levi, S., Salfeld, J., Franceschinelli, F., Cozzi, A., Doner, M.H., and Arosio, P. (1989) Expression and structural and functional properties of human ferritin L-chain from *Escherichia coli*. *Biochemistry* **28**, 5179–5184
14. Santambrogio, P., Levi, S., Arosio, P., Palagi, L., Vecchio, G., Lawson, D.M., Yewdall, S.J., Artymiuk, P.J., Harrison, P.M., Jappelli, R., and Cesareni, G. (1992) Evidence that a salt bridge in the light chain contributes to the physical stability difference between heavy and light human ferritins. *J. Biol. Chem.* **267**, 14077–14083
15. Hempstead, P.D., Yewdall, S.J., Fernie, A.R., Lawson, D.M., Artymiuk, P.J., Rice, D.W., Ford, G.C., and Harrison, P.M. (1997) Comparison of the three-dimensional structures of recombinant human H and horse L ferritins at high resolution. *J. Mol. Biol.* **268**, 424–448
16. Sano, K.-I., Ajima, K., Iwahori, K., Yudasaka, M., Iijima, S., Yamashita, I., and Shiba, K. (2005) Endowing a ferritin-like cage protein with high affinity and selectivity for certain inorganic materials. *Small* **1**, 826–832

17. Miura, A., Hikono, T., Matsumura, T., Yano, H., Hatayama, T., Uraoka, Y., Fuyuki, T., Yoshii, S., and Yamashita, I. (2006) Floating nanodot gate memory devices based on biomineralized inorganic nanodot array as a storage node. *Jpn. J. Appl. Phys.* **45**, L1–L3
18. Miura, A., Uraoka, Y., Fuyuki, T., Kumagai, S., Yoshii, S., Matsukawa, N., and Yamashita, I. (2007) Bionanodot monolayer array fabrication for nonvolatile memory application. *Surf. Sci.* **601**, L81–L85
19. Matsui, T., Matsukawa, N., Iwahori, K., Sano, K.-I., Shiba, K., and Yamashita, I. (2007) Realizing a two-dimensional ordered array of ferritin molecules directly on a solid surface utilizing carbonaceous material affinity peptides. *Langmuir* **23**, 1615–1618
20. Sano, K., Sasaki, H., and Shiba, K. (2006) Utilization of the pleiotropy of a peptidic aptamer to fabricate heterogeneous nanodot-containing multilayer nanostructures. *J. Am. Chem. Soc.* **128**, 1717–1722
21. Iwahori, K., Yoshizawa, K., Muraoka, M., and Yamashita, I. (2005) Fabrication of ZnSe nanoparticles in the apoferritin cavity by designing a slow chemical reaction system. *Inorg. Chem.* **44**, 6393–6400
22. Takeda, S., Ohta, M., Ebina, S., and Nagayama, K. (1993) Cloning, expression and characterization of horse L-ferritin in *Escherichia coli*. *Biochim. Biophys. Acta.* **1174**, 218–220
23. Okuda, M., Iwahori, K., Yamashita, I., and Yoshimura, H. (2003) Fabrication of nickel and chromium nanoparticles using the protein cage of apoferritin. *Biotechnol. Bioeng.* **84**, 187–194
24. Busch, M.R. and Ho, C.E. (1990) Effects of anions on the molecular basis of the Bohr effect of hemoglobin. *Biophys. Chem.* **37**, 313–322
25. Otwinowski, Z. and Minor, W. (1997) Processing of X-ray diffraction data collected in oscillation mode. *Methods Enzymol.* **276**, 307–326
26. Vagin, A.A. and Isupov, M.N. (2001) Spherically averaged phased translation function and its application to the search for molecules and fragments in electron-density maps. *Acta Crystallogr. D Biol. Crystallogr.* **57**, 1451–1456
27. Vagin, A. and Teplyakov, A. (2000) An approach to multi-copy search in molecular replacement. *Acta Crystallogr. D Biol. Crystallogr.* **56**, 1622–1624
28. Murshudov, G.N., Vagin, A.A., Lebedev, A., Wilson, K.S., and Dodson, E.J. (1999) Refinement of macromolecular structures by the maximum-likelihood method. *Acta Crystallogr. D Biol. Crystallogr.* **55**, 247–255
29. Roussel, A. and Cambillau, C. (1989) TURBO. in *Silicon Graphics Geometry Partner Directory* (Silicon Graphics Staff, ed.) pp. 77–78, Silicon Graphics, Mountain View, CA
30. Laskowski, R.A., McArthur, M.W., Moss, D.S., and Thornton, J.M. (1993) PROCHECK: a program to check the stereochemical quality of protein structures. *J. Appl. Crystallogr.* **26**, 283–291
31. Vriend, G. (1990) WHAT IF: a molecular modeling and drug design program. *J. Mol. Graph.* **8**, 52–56
32. Strickland, E. H. (1974) Aromatic contributions to circular dichroism spectra of proteins. *CRC Crit. Rev. Biochem.* **2**, 113–175
33. Listowsky, I., Betheil, J.J., and England, S. (1967) Conformation of ferritin and apoferritin in solution. Optical rotatory dispersion properties. *Biochemistry* **6**, 1341–1348
34. Fink, A.L., Calciano, L.J., Goto, Y., Kurotsu, T., and Palleros, D.R. (1994) Classification of acid denaturation of proteins: intermediates and unfolded states. *Biochemistry* **33**, 12504–12511